

Mössbauer study of nanodimensional nickel ferrite – mechanochemical synthesis and catalytic properties

E. Manova & C. Estournès & D. Paneva & J.-L. Reh & T. Tsoncheva & B. Kunev & I. Mitov
E. Manova : D. Paneva : B. Kunev : I. Mitov
Institute of Catalysis, Bulgarian Academy of Sciences,
Acad. G. Bonchev Str., bl. 11, 1113 Sofia, Bulgaria

T. Tsoncheva
Institute of Organic Chemistry, Bulgarian Academy of Sciences,
Acad. G. Bonchev Str., bl. 9, 1113 Sofia, Bulgaria

J.-L. Reh
I.P.C.M.S. Groupe des Matériaux Inorganiques, UMR7504 CNRS, ULP, ECPM.,
23 rue du Loess, BP 43, 67034 Strasbourg Cedex 2, France

C. Estournès (*)
CIRIMAT, UMR5085 CNRS, UPS,
118, route de Narbonne, 31062 Toulouse Cedex 4, France
e-mail: estourne@chimie.ups-tlse.fr

Abstract

Iron–nickel spinel oxide NiFe₂O₄ nanoparticles have been prepared by the combination of chemical precipitation and subsequent mechanical milling. For comparison, their analogue obtained by thermal synthesis is also studied. Phase composition and structural properties of iron–nickel oxides are investigated by X-ray diffraction and Mössbauer spectroscopy. Their catalytic behavior in methanol decomposition to CO and methane is tested. An influence of the preparation method on the reduction and catalytic properties of iron–nickel samples is established.

Key words : X-ray diffraction . Mössbauer spectroscopy . mechanochemical synthesis . methanol decomposition, ferrite nanoparticles

1 Introduction

The synthesis of spinel ferrite nanoparticles has been intensively studied in the recent years, because of their large-scale application. The principal role of the preparation conditions on the morphological and structural features of the ferrites is discussed [1–6]. In the last two

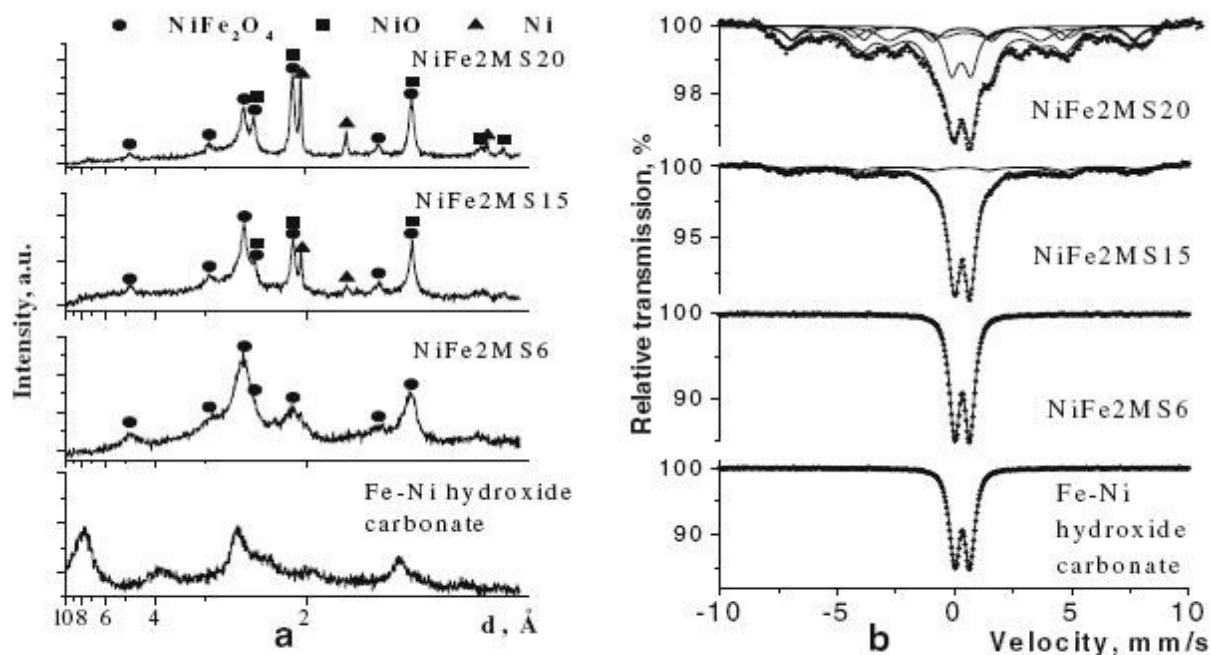


Figure 1 XRD patterns (a, abscissa is d-spacing) and Mössbauer spectra (b) of the samples before and after different milling times.

decades, the decomposition of methanol to CO and H₂ has received growing attention because of its possible use as an alternative, ecological fuel. The reaction is also applicable to the recovery of waste heat from industries, but significant improvement of the catalysts must be achieved. In our previous studies [7] it was shown that nanosized cobalt ferrites present a good activity in methanol decomposition, and both the preparation method and Fe/Co ratio influence the phase transformations and catalytic behavior of the samples. The present paper aims at studying the effects of the preparation method on the catalytic properties in methanol decomposition of nanosized nickel ferrites obtained by mechanochemical and thermal methods.

2 Experimental

The starting materials used were Fe(NO₃)₃·9H₂O (purity 99%), Ni(NO₃)₂·6H₂O (purity 96%) and Na₂CO₃. Nickel ferrite powders (NiFe₂O₄) were prepared in two steps: (1) co-precipitation to obtain the precursor, and (2) mechanical milling of the precursor. For the co-precipitation the procedure described in [7] was followed. The obtained precursor powders were milled using a Fritsch Planetary miller in a hardened steel vial together with fifteen grinding balls having different diameters (ranging from 3 to 10 mm). The ball-to-powder mass charge ratio was 10:1. The powders were milled for 6, 15 and 20 h (samples denoted as NiFe2MS6, NiFe2MS15 and NiFe2MS20, respectively).

The thermal synthesis (NiFe2TS) was performed as described in [7].

Phase composition and structural properties of the obtained samples are investigated by X-ray diffraction (XRD) and Mössbauer spectroscopy. The powder XRD patterns were recorded by use of a TUR M62 diffractometer with Co K α radiation. The observed patterns were cross-matched with those in the JCPDS database. Mössbauer spectra of nanosize nickel ferrite particles were recorded at 295 K on a Wissel electromechanical Mössbauer

spectrometer (Wissenschaftliche Elektronik GmbH, Germany) working in a constant acceleration mode. A $^{57}\text{Co}/\text{Cr}$ (activity $\cong 10$ mCi) source and an α -Fe standard were used.

Table I Mössbauer parametra of mecanochemically synthesized samples

Sample	Components	IS (mm/s)	QS (mm/s)	H_{eff} (kOe)	FWHM (mm/s)	G (%)
NiFe2MS6	SPM $\text{NiFe}_2\text{O}_4 - \text{Fe}^{3+}_{\text{octa}}$	0.33	0.67	–	0.50	100
NiFe2MS6	$\text{Fe}_3\text{O}_4 - \text{Fe}^{3+}_{\text{tetra}}$	0.29	0.03	485	0.48	19
after catalytic test	$\text{Fe}_3\text{O}_4 - \text{Fe}^{2.5+}_{\text{octa}}$	0.71	0.01	457	0.63	17
	Fe-Ni	0.01	0.04	307	0.68	44
	Fe_3C	0.21	0.03	197	0.44	20
NiFe2MS15	$\text{NiFe}_2\text{O}_4 - \text{Fe}^{3+}_{\text{tetra}}$	0.26	0.00	435	1.00	15
	$\text{NiFe}_2\text{O}_4 - \text{Fe}^{3+}_{\text{octa}}$	0.36	0.00	476	1.00	12
	SPM $\text{NiFe}_2\text{O}_4 - \text{Fe}^{3+}$	0.33	0.70	–	0.63	73
NiFe2MS20	$\text{NiFe}_2\text{O}_4 - \text{Fe}^{3+}_{\text{tetra}}$	0.25	0.00	435	1.26	13
	$\text{NiFe}_2\text{O}_4 - \text{Fe}^{3+}_{\text{octa}}$	0.35	0.00	476	0.50	42
	Fe-Ni	0.12	0.10	289	0.50	14
	SPM $\text{NiFe}_2\text{O}_4 - \text{Fe}^{3+}$	0.33	0.65	–	0.50	28
	Fe^{2+}	0.86	2.33	–	0.40	3
NiFe2MS20	$\text{Fe}_3\text{O}_4 - \text{Fe}^{3+}_{\text{tetra}}$	0.28	0.00	478	0.52	18
after catalytic test	$\text{Fe}_3\text{O}_4 - \text{Fe}^{2.5+}_{\text{octa}}$	0.55	0.00	441	0.74	13
	Fe-Ni	0.02	0.00	306	0.70	60
	Fe_3C	0.18	0.04	189	0.46	9
NiFe2TS	$\text{NiFe}_2\text{O}_4 - \text{Fe}^{3+}_{\text{tetra}}$	0.26	0.00	464	0.78	57
	$\text{NiFe}_2\text{O}_4 - \text{Fe}^{3+}_{\text{octa}}$	0.36	0.00	500	0.71	43
NiFe2TS	$\text{NiFe}_2\text{O}_4 - \text{Fe}^{3+}_{\text{tetra}}$	0.26	0.00	492	0.28	15
after catalytic test	$\text{NiFe}_2\text{O}_4 - \text{Fe}^{3+}_{\text{octa}}$	0.36	0.00	510	0.45	24
	$\text{Fe}_3\text{O}_4 - \text{Fe}^{3+}_{\text{tetra}}$	0.28	0.00	483	0.26	10
	$\text{Fe}_3\text{O}_4 - \text{Fe}^{2.5+}_{\text{octa}}$	0.61	0.00	457	0.42	12
	Fe-Ni	0.15	0.08	299	0.50	27
	Fe_3C	0.18	0.02	205	0.40	12

The experimental spectra were treated using the least squares method. The parameters of hyperfine interaction such as isomer shift (IS), quadrupole splitting (QS) and effective internal magnetic field (H_{eff}) as well as the line widths (FWHM) and the relative weight (G) of the partial components of the spectra were determined.

The catalytic experiments were performed in a fixed-bed reactor (0.1 g catalyst) at a methanol partial pressure of 1.57 kPa and a WHSV of 1.5 h⁻¹. The temperature was raised with a rate of 1 K/min in the range of 350–723 K. The on-line gas chromatographic analysis was made on a Porapak Q and a molecular sieve column using an absolute calibration method [8].

3 Results and discussion

XRD patterns of the precursor and those after different milling times are shown in Figure 1. The pattern of the precursor is characteristic of layered double hydroxides as found for pyroaurite (PDF 25-0521) and hydrotalcite (PDF 41-1428). After 6 h of milling the diffraction pattern of the sample consists of broad peaks. Their position and intensities suggest the formation of a spinel phase with cubic structure and lattice constant $a_0 = 8.341 \text{ \AA}$, corresponding to NiFe_2O_4 .

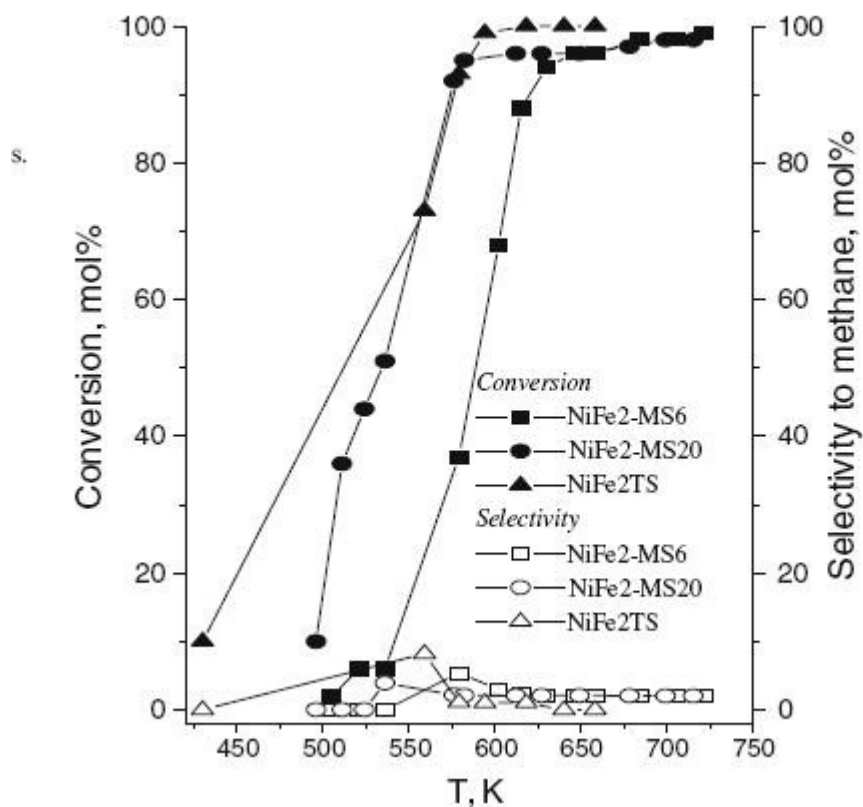


Figure 2 Temperature dependencies of methanol conversion and methane selectivity for mechanochemically and thermally synthesized nickel ferrites.

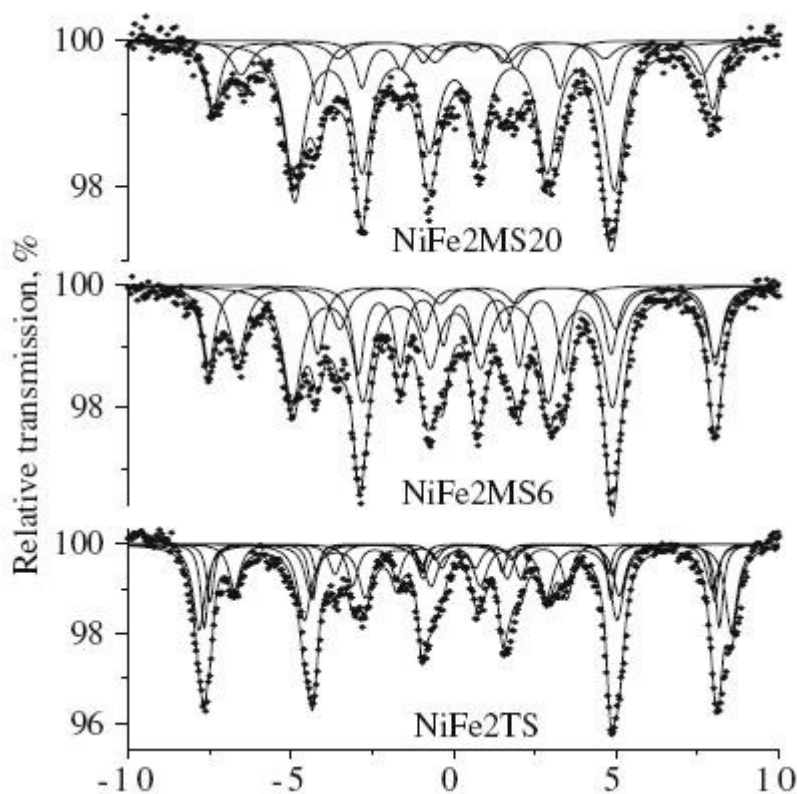


Figure 3 Mössbauer spectra of the samples after catalytic test.

The diffraction patterns show that with the increase of milling time some decomposition of the spinel phase into Ni and FeNi alloy occur. The average particle size calculated by the Scherrer equation is 3.5, 5.2 and 8.1 nm for NiFe2MS6, NiFe2MS15 и NiFe2MS20, respectively. It is interesting to note that the process of crystallization continues as a function of treatment time and at later stages is accompanied by the reduction to nickel. In our previous study we evidenced that high-energy milling of cobalt ferrite spinels in a steel vial and using steel balls induces the reduction of cobalt ions to metallic cobalt [9].

Mössbauer spectroscopy was applied to obtain more information about the phase composition, cationic occupations and/or different state distribution of iron ions in the studied ferrite materials. Figure 1b shows the RT Mössbauer spectra of samples taken from different steps of the processing route. The corresponding parameters are listed in Table I. The co-precipitated precursor exhibits a quadrupole doublet with $IS=0.33$ mm/s, $QS=0.65$ mm/s, indicating that the hydroxide carbonate precursor is paramagnetic. As shown in Figure 1b the spectrum of NiFe2MS6 presents a doublet. The spectra of NiFe2MS15 and NiFe2MS20 consist of a central doublet superposed on a sextet pattern. A considerable diminution of the doublet component for the spectrum of NiFe2MS20 is observed. The doublets observed in all milled samples arise from Fe(III)-ions in ultradispersed ferrite particles exhibiting superparamagnetic (SPM) behavior [10, 11]. This particle size effect is in good agreement with the XRD data.

In Figure 2 the temperature dependencies of methanol conversion and methane selectivity for mechanochemically and thermally synthesized nickel ferrites are shown. Total (100%) methanol conversion is registered just above 575 K for NiFe2TS and NiFe2MS20, and at about 625 K for NiFe2MS6. CO and H₂ are the main products in all cases. Different degrees

of phase transformations in mechanochemically and thermally synthesised samples during the catalytic test are found. The presence of Ni-doped Fe₃O₄, NiFe alloy and Fe₃C is observed for the all studied samples (Figure 3, Table I), but in the case of NiFe₂TS a significant amount of unchanged ferrite phase is also found. The formation of iron–cobalt alloys and iron carbides after catalytic test is found for the mechanosynthesized CoFe₂O₄ too and is correlated with the observed low selectivity to methane [7].

4 Conclusion

The high-energy ball milling of the layered nickel–iron hydroxide carbonates results in the formation of nanocrystalline nickel ferrite, where the particle size can be controlled by the treatment time. Differences in the phase composition and catalytic behavior in methanol decomposition of nickel ferrites are observed depending on the preparation method used. Both, the variations in the phase composition and the particles dispersion affect the catalytic properties of the samples.

Acknowledgments The authors thank the National Science Fund of the Bulgarian Ministry of Education and Science for the financial support of Project X-1504/05.

References

1. Shaft, K.V.P.M., Gedanken, A.: *Chem. Mater.* 10, 3445 (1998)
2. Kim, C.S., Yi, Y.S.: *J. Appl. Phys.* 85, 5223 (1999)
3. Kim, Y.J., Kim, D., Lee, C.S.: *Physica B* 337, 42 (2003)
4. Shi, Y., Ding, J., Liu, X., Wang, J.: *J. Magn. Magn. Mater.* 205, 249 (1999)
5. Lee, S., John, V.T., O'Connor, C., Harris, V., Carpenter, E.: *J. Appl. Phys.* 87, 6223 (2000)
6. DeGuede, M.R., O'Handley, R.C., Kaionji, G.: *J. Appl. Phys.* 65, 3167 (1989)
7. Manova, E., Tsoncheva, T., Paneva, D., Mitov, I., Tenchev, K., Petrov, L.: *Appl. Catal., A General* 277, 119 (2004)
8. Tsoncheva, T., Dimitrov, M., Paneva, D., Mitov, I., Köhn, R., Fröba, M., Minchev, Ch.: *React. Kinet. Catal. Lett.* 74, 385 (2001)
9. Manova, E., Kunev, B., Paneva, D., Mitov, I., Petrov, L., Estournès, C., d'Orléans, C., Reh, J.L., Kurmoo, M.: *Chem. Mater.* 16, 5689 (2004)
10. Shi, Y., Ding, J., Yin, H.: *J. Alloys Compd.* 308, 290 (2000)
11. Ahn, Y., Choi, E.J., Kim, S., Ok, H.N.: *Mater. Lett.* 50, 47 (2001)

